Photoisomerization Efficiency in UV-Absorbing Visual Pigments: Protein-Directed Isomerization of an Unprotonated Retinal Schiff Base†

Kei Tsutsui, Hiroo Imai,‡ and Yoshinori Shichida*

Department of Biophysics, Graduate School of Science, Kyoto University, Kyoto 606-8502, Japan, and CREST, Japan Science and Technology Agency, Kyoto, Japan

Received February 23, 2007; Revised Manuscript Received March 22, 2007

ABSTRACT: A visual pigment consists of an opsin protein and a chromophore, 11-*cis*-retinal, which binds to a specific lysine residue of opsin via a Schiff base linkage. The Schiff base chromophore is protonated in pigments that absorb visible light, whereas it is unprotonated in ultraviolet-absorbing visual pigments (UV pigments). To investigate whether an unprotonated Schiff base can undergo photoisomerization as efficiently as a protonated Schiff base in the opsin environment, we measured the quantum yields of the bovine rhodopsin E113Q mutant, in which the Schiff base is unprotonated at alkaline pH, and the mouse UV pigment (mouse UV). Photosensitivities of UV pigments were measured by irradiation of the pigments followed by chromophore extraction and HPLC analysis. Extinction coefficients were estimated by comparing the maximum absorbances of the original pigments and their acid-denatured states. The quantum yield of the bovine rhodopsin E113Q mutant at pH 8.2, where the Schiff base is unprotonated, was significantly lower than that of wild-type rhodopsin, whereas the mutant gave a quantum yield almost identical to that of the wild type at pH 5.5, where the Schiff base is protonated. These results suggest that Schiff base protonation plays a role in increasing quantum yield. The quantum yield of mouse UV, which has an unprotonated Schiff base chromophore, was significantly higher than that of the unprotonated form of the rhodopsin E113Q mutant, although it was still lower than the visible-absorbing pigments. These results suggest that the mouse UV pigment has a specific mechanism for the efficient photoisomerization of its unprotonated Schiff base chromophore.

The visual transduction cascade in photoreceptor cells begins with photon absorption by visual pigments. A visual pigment consists of a protein moiety, opsin, and a chromophore, 11-*cis*-retinal, which covalently binds to K296[1] in transmembrane helix 7 of the opsin via a Schiff base linkage (Figure 1). Light photoisomerizes the chromophore from 11-*cis* to its all-*trans* form (*1*, *2*). This reaction takes place on an ultrafast time scale (<200 fs) (*3*). The photoisomerization leads to structural changes of the opsin driving it toward its active form, and this in turn leads to the activation of the G protein-mediated signal transduction cascade which eventually generates an electrical response of the photoreceptor cells (*4*).

Vertebrate visual pigments can be classified into five groups on the basis of their sequence similarities; L (LWS/MWS), S (SWS1), M1 (SWS2), M2 (RH2), and rhodopsins (RH1) (*5*−*7*). This classification is in good agreement with the classification based on the λ_{max}.[2] However, the S group contains two types of visual pigments which differ in their λ_{max}. One has its λ_{max} in the violet region (390−440 nm), and the other has its λ_{max} in the UV region (around 360 nm).

It was proposed that the Schiff base of the chromophore of UV pigments is in its unprotonated form (*8*) (Figure 1B), as opposed to that of the visible-absorbing pigments such as bovine rhodopsin where the Schiff base is in its protonated form (*9*, *10*) (Figure 1A). Several lines of evidence that support this hypothesis (*11*, *12*) have been reported since the first report in 1998 of the successful expression of UV pigments in cultured-cell systems (*13*−*15*). Fasick et al. (*11*) reported that the λ_{max} of mouse UV pigment (mouse UV; 358 nm) was shifted to 424 nm when phenylalanine at position 86 was substituted with tyrosine (F86Y), and the double mutation (F86Y/E113Q) caused a pH-dependent shift of the λ_{max}. These results suggested that the Schiff base chromophore in mouse UV was protonated by the F86Y mutation and the protonation state was stabilized by E113 as the "counterion" (*11*). FTIR spectroscopy also demonstrated that the chromophore of mouse UV is unprotonated (*12*).

† This work was supported in part by Grants-in-Aid for Scientific Research, Priority Areas (15770097), and a Grant for Biodiversity Research of the 21st Century COE (A14) from the Japanese Ministry of Education, Culture, Sports, Science, and Technology to Y.S.

* Corresponding author. Telephone: +81-75-753-4213. Fax: +81-75-753-4210. E-mail: shichida@vision-kyoto-u.jp.

‡ Present address: Department of Cellular and Molecular Biology, Primate Research Institute, Kyoto University, Inuyama, Aichi 484-8506, Japan.

[1] The numbers of all amino acid residues in this paper are based on the bovine rhodopsin numbering system.

[2] Abbreviations: λ_{max}, wavelength at the absorption maximum; UV, ultraviolet; UV pigment, ultraviolet-absorbing visual pigment; FTIR, Fourier transform infrared spectroscopy; DM, dodecyl β-D-maltoside; HEPES, *N*-(2-hydroxyethyl)piperazine-*N*′-2-ethanesulfonic acid; MES, 2-morpholinoethanesulfonic acid; 13s, 13-*cis*-15-*syn*-retinaloxime; 13a, 13-*cis*-15-*anti*-retinaloxime; 11s, 11-*cis*-15-*syn*-retinaloxime; 11a, 11-*cis*-15-*anti*-retinaloxime; 9s, 9-*cis*-15-*syn*-retinaloxime; 9a, 9-*cis*-15-*anti*-retinaloxime; Ts, *all-trans*-15-*syn*-retinaloxime; Ta, *all-trans*-15-*anti*-retinaloxime.

10.1021/bi7003763 CCC: $37.00
Published on Web 05/03/2007

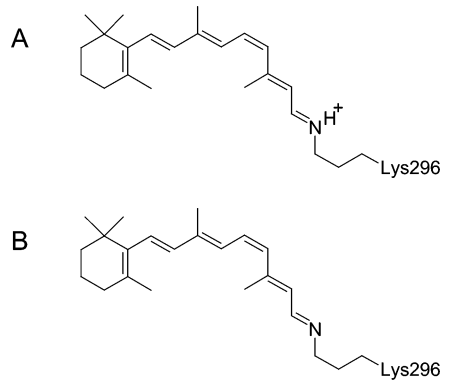

FIGURE 1: Retinal Schiff base choromophores. (A) Protonated 11-*cis*-retinal Schiff base, the chromophore of wild-type bovine rhodopsin, and the protonated form (pH 5.5) of the E113Q mutant. (B) Unprotonated 11-*cis*-retinal Schiff base, the chromophore of mouse UV, and the unprotonated form (pH 8.2) of the rhodopsin E113Q mutant.

The discovery that UV pigments have an unprotonated Schiff base raises an important question: Is the Schiff base proton needed only to allow pigments to shift their spectrum so that they can absorb visible light? Or are there other costs in using an unprotonated Schiff base chromophore? For example, electronic states of an unprotonated Schiff base should be quite different from those of the protonated form because of less π-electron delocalization, and this may perturb photochemical aspects of the retinal chromophore, such as its efficiency of photoisomerization (*16*, *17*). At the same time, the efficiency of photoisomerization of a retinal chromophore in its protein environment is determined not only by the intrinsic properties of retinal but also by the interaction between the chromophore and its protein moiety. In fact, the quantum yield of the protonated retinal Schiff base in rhodopsin, 0.65 (*18*) [a recently refined value from the long-accepted one, 0.67 (*19*)], is 2−4 times higher than that of the protonated retinal Schiff base in solution (0.18−0.23) (*20*), indicating that the protein facilitates photoisomerization (*21*, *22*). Therefore, we were interested in determining the quantum yield of UV pigments.

In the present study, we report the quantum yields of two different UV pigments. One is the Schiff base counterion mutant of bovine rhodopsin (E113Q), where the Schiff base is unprotonated at high pH (*23*−*25*). The other is mouse UV, where the Schiff base is unprotonated in its normal state. The photosensitivities of visible-absorbing pigments are usually measured by monitoring the decrease of its absorbance at its absorption maximum as a function of irradiation time in the presence of hydroxylamine (*19*, *26*). However, this method cannot be applied to UV pigments, because the absorption spectrum of the photoproduct significantly overlaps that of the unphotolyzed pigment. So the photosensitivities of UV pigments were estimated by analyzing the isomeric composition of the photoproducts using HPLC. The results showed that the quantum yield of the unprotonated form of the rhodopsin E113Q mutant was much lower than that of the protonated form and of the wild-type pigment. On the other hand, mouse UV, though lower than the visible-absorbing pigments, exhibited a significantly higher quantum yield than the unprotonated form of the rhodopsin E113Q mutant. These results suggest that mouse UV has a specific mechanism for the efficient photoisomerization of its unprotonated Schiff base chromophore.

MATERIALS AND METHODS

Sample Preparation. Opsins were expressed in the HEK 293T cell lines as previously reported (*27*, *28*). For the purpose of purification, the cDNA of mouse UV was tagged by the monoclonal antibody Rho1D4 epitope sequence (8 aa C-terminal of bovine rhodopsin; ETSQVAPA) (*29*). The cDNA of the bovine rhodopsin E113Q mutant was derived from the previous study (*30*). The wild-type and mutant cDNAs were fully sequenced before being introduced into the expression vector, pUSRα (*31*) for bovine rhodopsin and pcDLSRα 296 (*32*) for mouse UV.

To reconstitute photoreactive pigments, the expressed opsins were incubated with 11-*cis*-retinal for more than 3 h at 4 °C. The pigments were extracted with buffer A [1% (w/v) dodecyl β-D-maltoside (DM), 25 mM HEPES, 70 mM NaCl, and 1.5 mM $MgCl_2$, pH 6.5 at 3 °C]. The extracted pigments were then purified by adsorbing them on an antibody-conjugated column (*30*) and then eluted by buffer B (0.3 mg/mL 1D4 peptide, 0.02% DM, 50 mM HEPES, 140 mM NaCl, and 3 mM $MgCl_2$, pH 6.5), buffer C (0.3 mg/mL 1D4 peptide, 0.02% DM, 50 mM HEPES, 140 mM NaCl, and 3 mM $MgCl_2$, pH 8.2), or buffer D (0.3 mg/mL 1D4 peptide, 0.02% DM, 50 mM MES, 140 mM NaCl, and 3 mM $MgCl_2$, pH 5.5). All procedures were done under dim red light. Eluted samples were kept at −80 °C until use.

Photosensitivities of the Protonated Form of the Rhodopsin E113Q Mutant. For the photosensitivity measurement of the protonated form of the rhodopsin E113Q mutant, the conventional method (*18*, *19*, *26*) was used. Briefly, the sample (0.086 ± 0.015 OD, 250 μL) was supplemented with 12.5 μL of hydroxylamine chloride solution (pH 5.5, 100 mM) and put in a cuvette (width, 2 mm; light path, 1 cm). The cuvette was then put in the cell holder of a UV−vis spectrophotometer (Hitachi U-4100) and kept at 3 °C by using a temperature controller (Thermo Neslab RTE-7) during the experiment. The sample was incubated for ∼15 h, and absorption spectra were measured at 30 min intervals in order to estimate the rate constant of dark bleaching due to hydroxylamine. Then the photosensitivity was measured using the same sample. The sample was successively irradiated with light from a 1 kW tungsten halogen lamp (Master HILUX-HR; Rikagaku) which had been passed through an interference filter (500 nm; half-bandwidth, 5 nm; Optical Coatings Japan), and the absorbance change was monitored. The light intensity was attenuated by using neutral-density filters, so that irradiation for 30 min caused bleaching of ∼90% of wild-type rhodopsin, so our conditions were comparable to those of Dartnall (*19*). After every irradiation (2.5 min × 8 times followed by 5 min once), the sample was incubated for 40−80 min until any small amounts of residual photointermediates were completely converted to retinaloximes. Finally, the sample was completely bleached by intense >500 nm light which had been passed through a cutoff filter (VY52; Toshiba). The amount of residual pigment after every irradiation, after a correction for dark bleaching of the pigment due to hydroxylamine, was calculated as described in Supporting Information.

The photon number (s^{-1}•cm^{-2}) of the irradiation light was calculated from the power (W) of the irradiation light measured by a power meter (PM-245; Neoark). The intensity of the incident light was continuously monitored by a photodiode (S1226-5BQ; Hamamatsu Photonics) attached in front of the cell holder, and the data were transferred to a data acquisition system (Powerlab 2/20; ADInstruments). A correction was made for the fluctuation of the light intensity as monitored by the photodiode system.

The calculated amounts of the residual pigment were plotted on a semilogarithmic scale against the incident photon flux and fitted with an exponential function. The slope of the fitting line corresponds to the relative photosensitivity of the pigment at the irradiating wavelength (*19*, *26*). For every measurement, the photosensitivity of wild-type rhodopsin was measured at the same time as a control, and the photosensitivity of the E113Q mutant was determined as a relative value to that of the wild type. For the measurement of the wild type, hydroxylamine chloride solution (pH 6.5, 1 M) was used.

Photosensitivities of the Unprotonated Form of the Rhodopsin E113Q Mutant and Mouse UV. The method for photosensitivity measurement which was described above cannot be applied to the unprotonated form (pH 8.2) of the rhodopsin E113Q mutant and mouse UV, because the absorption spectrum of retinaloxime significantly overlaps that of the unphotolyzed pigment. So the photosensitivities of these pigments were measured by the following method. The photosensitivity of the protonated form (pH 5.5) of the rhodopsin E113Q mutant was also measured to confirm the reliability of the method.

First, a single sample (0.025 ± 0.005 OD, 1 mL) was divided into four aliquots. Then a 12.5 μL aliquot of hydroxylamine sulfate (pH 8.2, 50 mM), hydroxylamine chloride (pH 6.5, 200 mM), or hydroxylamine chloride (pH 5.5, 100 mM) was added to the sample of the unprotonated form, mouse UV, or the protonated form, respectively. For the unprotonated form, hydroxylamine sulfate was used instead of hydroxylamine chloride, because chloride ion stabilizes the Schiff base proton in the E113Q mutant (*33*).

The cuvette containing the sample was put in the cell holder of the spectrophotometer and irradiated as described above. The interference filters' wavelengths (Optical Coatings Japan) were centered at 390 nm (half-bandwidth, 10 nm), 359 nm (half-bandwidth, 11 nm), or 500 nm (half-bandwidth, 5 nm) for the unprotonated form, mouse UV, or the protonated form, respectively. Each aliquot was irradiated for 0, 5, 10, and 20 min, respectively. To prevent accumulation of photointermediates, samples were incubated for 20 min after every 5 min irradiation. The photointermediates of the protonated form were relatively stable, so the irradiated samples were incubated for 50−80 min. In every experiment, wild-type rhodopsin was irradiated at the same time as a reference.

The chromophores were then extracted from the irradiated aliquots as retinaloximes as previously described (*34*, *35*). Briefly, the sample was collected from the cuvette after irradiation and placed on ice. Hydroxylamine was added to the sample (final concentration, 91 mM). After 10 min incubation on ice, the sample was supplemented with methanol (250 μL) and dichloromethane (250 μL) and mixed thoroughly with a Pasteur pipet to denature the pigment. Hexane (1 mL) was added to the sample, followed by mixing with a pipet to transfer the retinaloximes to the hexane layer. After centrifugation with a hand-operated centrifuge, the hexane layer was collected. This hexane extraction was repeated once more. The collected hexane layer was dried over anhydrous Na_2SO_4 and then evaporated under a N_2 stream. All procedures were done under dim red light. The sample was stored at −80 °C until use.

The isomeric composition of the extracted retinaloxime was analyzed by HPLC (LC-10AT VP; Shimadzu) equipped with a silica column (150 × 6.0 mm, A-012-3; YMC). The solvent was composed of 98.8% (v/v) benzene, 1.0% (v/v) diethyl ether, and 0.2% (v/v) 2-propanol (*34*−*36*), and the flow rate was 1.0 mL/min. Dried samples were dissolved in 20 μL of hexane, and 10 μL was used for HPLC analysis. The HPLC patterns were obtained by monitoring the absorbance at 360 nm. Before every experiment, a sample containing authentic *syn* and *anti* isomers of 11-*cis*-, 9-*cis*-, 13-*cis*-, and *all*-*trans*-retinaloximes was subjected to the HPLC to assign the retention time of each isomer. The isomeric composition of the sample was calculated from the areas of the peaks and the molar extinction coefficients at 360 nm (*37*): 13s, 49000; 13a, 52100; 11s, 35000; 11a, 29600; 9s, 39300; 9a, 30600; Ts, 54900; Ta, 51600. After correction for dark bleaching, the amounts of the residual pigment were calculated from the percentages of the 11-*cis* isomer in the samples (see Supporting Information) and were plotted on a semilogarithmic scale against the incident photon numbers and fitted with a single exponential function to estimate the photosensitivity.

Molar Extinction Coefficients. The molar extinction coefficients of the pigments were determined by the acid denaturation method (*24*, *38*) as follows: After recording the dark-state spectrum, we added 14 μL (10 μL for pH 5.5 samples, 18 μL for pH 8.2 samples) of 2 N HCl to the sample (final pH, 1.3 ± 0.2). Addition of HCl denatured the pigment and trapped the chromophore as a protonated Schiff base with a λ_{max} of ∼440 nm. Any visual pigments investigated in the present study gave spectrally identical species upon acid denaturation, so that we were able to estimate the molar extinction coefficients of pigments by comparing the ratio of the maximum absorbance before and after denaturation by HCl with that obtained from bovine rhodopsin [molar extinction coefficient, 40600 M^{-1} cm^{-1} (*39*)]. In this method light scatter at shorter wavelengths would significantly distort the results, so we used samples with relatively high absorbance (0.051 ± 0.003) to reduce any error from the scattering effect. The spectra after an addition of HCl were corrected for dilution.

Quantum Yields. Using the separately determined values of molar extinction coefficients and photosensitivities, the quantum yields (ϕ) of visual pigments were calculated using the relationship (*18*, *19*, *26*):

$$S \propto \epsilon\phi$$

where S and ϵ are the photosensitivity and the molar extinction coefficient. The values of quantum yields were estimated relative to that of wild-type bovine rhodopsin [0.65 (*18*)].

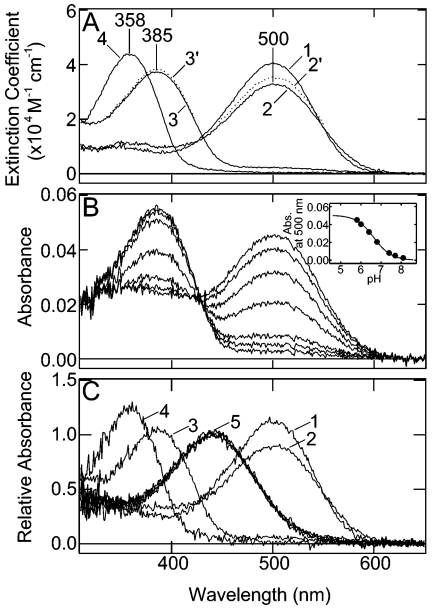

FIGURE 2: Absorption spectra of the visual pigments. (A) Absorption spectra of wild-type bovine rhodopsin (curve 1), the E113Q mutant (curve 2, pH 5.5; curve 3, pH 8.2), and mouse UV (curve 4) at 3 °C are shown. 2′ and 3′ (broken lines) are the spectra where 100% protonated and unprotonated forms are assumed, respectively. The λ_{max} values are indicated in each spectrum. (B) Absorption spectra of the rhodopsin E113Q mutant at pH 8.1, 7.7, 7.4, 6.8, 6.4, 6.0, and 5.8 (in order of increasing absorbance at 500 nm). Inset: Plot of the absorbance at 500 nm against pH and a fitting with a Henderson−Hasselbalch equation. The average pK_a value calculated from four independent experiments was 6.6 ± 0.1. (C) Typical absorption spectra before and after acid denaturation. Curves 1−4 are absorption spectra of wild-type rhodopsin (curve 1), the E113Q mutant (curve 2, pH 5.5; curve 3, pH 8.2), and mouse UV (curve 4) before acid denaturation. All of these pigments gave species that were spectrally the same with a λ_{max} of 440 nm (curve 5) upon acid denaturation so that the determination of the molar extinction coefficients was possible. The same experiments were repeated at least four times for each pigment. Then the extinction coefficients of the visual pigments were calculated using the value for bovine rhodopsin, 40600 M^{-1} cm^{-1} (*39*). Taking into account the ratio of the protonated and the unprotonated forms at pH 5.5 and pH 8.2 determined with a pK_a of 6.6 ± 0.1, the extinction coefficients of the protonated and the unprotonated forms were determined as 35600 ± 1000 and 38100 ± 1000 M^{-1} cm^{-1} at the irradiation wavelengths (500 and 390 nm), respectively. The extinction coefficient of mouse UV was 43600 ± 1200 M^{-1} cm^{-1} at the irradiation wavelength (359 nm).

RESULTS

Absorption Spectra of Visual Pigments. The λ_{max} of the bovine rhodopsin E113Q mutant was 500 nm at pH 5.5 (curve 2 in Figure 2A) and 385 nm at pH 8.2 (curve 3 in Figure 2A), as previously reported (*23*−*25*). The two peaks correspond to the two different states of the Schiff base, protonated and unprotonated (Figure 1). We shall call the two states of the rhodopsin E113Q mutant "the protonated form" and "the unprotonated form", respectively. The sample contained almost exclusively the protonated form at pH 5.5, although a small amount of the unprotonated form appeared to be present (and vice versa at pH 8.2). To determine the proportion of the protonated form at each pH, the pK_a value of Schiff base protonation was determined by changing the pH of the solution and plotting absorbance at 500 nm, followed by fitting with a Henderson−Hasselbalch equation (Figure 2B and inset). The average value of four independent experiments was 6.6 ± 0.1, which was similar to that reported previously (*40*). The percentages of the protonated form calculated using the pK_a value were 93 ± 2% and 2.5 ± 0.5% at pH 5.5 and 8.2, respectively. Mouse UV had its λ_{max} at 358 nm (curve 4 in Figure 2A), as previously reported (*11*, *12*, *14*).

We then determined the molar extinction coefficients of the pigments using the acid denaturation method (Figure 2C). The pigments were acid denatured, and the ratio of peak absorbance before and after the acid denaturation was compared to that of wild-type rhodopsin. Using the molar extinction coefficient of rhodopsin at 500 nm [40600 M^{-1} cm^{-1} (*39*)], the molar extinction coefficient at the peak of the pigment was obtained. At least four experiments were performed for each pigment. Considering the percentages of the protonated form determined above, the molar extinction coefficients of the protonated and the unprotonated form were estimated to be 35600 ± 1000 and 38100 ± 1000 M^{-1} cm^{-1} at the irradiation wavelengths (the protonated form, 500 nm; the unprotonated form, 390 nm), respectively. The molar extinction coefficient of mouse UV was estimated to be 43600 ± 1200 M^{-1} cm^{-1} at the irradiation wavelength (359 nm).

Quantum Yield of the Protonated Form of the Rhodopsin E113Q Mutant. First, the photosensitivity of the protonated form of the rhodopsin E113Q mutant was measured by the conventional method.

Before a photosensitivity measurement, the sample was incubated for ∼15 h in the presence of 4.8 mM hydroxylamine to estimate the rate of dark bleaching (data not shown). The rate constant of dark bleaching was (1.4 ± 1.2) × 10^{-4} min^{-1} (n = 4). The value for wild-type rhodopsin in the presence of 48 mM hydroxylamine was (3.9 ± 2.7) × 10^{-5} min^{-1} (n = 4). These values were used in the correction to the photobleaching data (see Supporting Information).

The sample was then successively irradiated with 500 nm light, and the absorbance change was monitored (Figure 3A). The photosensitivity of the wild-type pigment was measured at the same time for each experiment (Figure 3B). After correction for dark bleaching, the amounts of residual pigment were plotted on a semilogarithmic scale against the incident photon flux and fitted with an exponential function (Figure 3F). The photosensitivity of the mutant, which was obtained as the slope of the fitting line, was 0.87 ± 0.02 (n = 4) relative to the wild type. This value and the extinction coefficient at 500 nm (35600 ± 1000 M^{-1} cm^{-1}) gave the quantum yield of 0.65 ± 0.02, which was almost identical to that of the wild type [0.65 (*18*)].

The photosensitivity of the protonated form was also measured by another method, chromophore extraction and HPLC analysis. The samples were divided into four aliquots. Each was then supplemented with hydroxylamine (final concentration, 4.8 mM) and irradiated for 0, 5, 10, or 20 min with 500 nm light. Chromophores were extracted from the irradiated samples as retinaloximes and were subjected to HPLC analysis (Figure 3C−E). The results showed that the photoisomerization of the chromophore from 11-*cis* to all-*trans* form took place as a function of irradiation time, while the small amount of 9-*cis* and 13-*cis* isomers (<5% in total) was present in the extracts. These isomers were probably derived from the all-*trans* isomer through thermal isomerization in the course of chromophore extraction. The

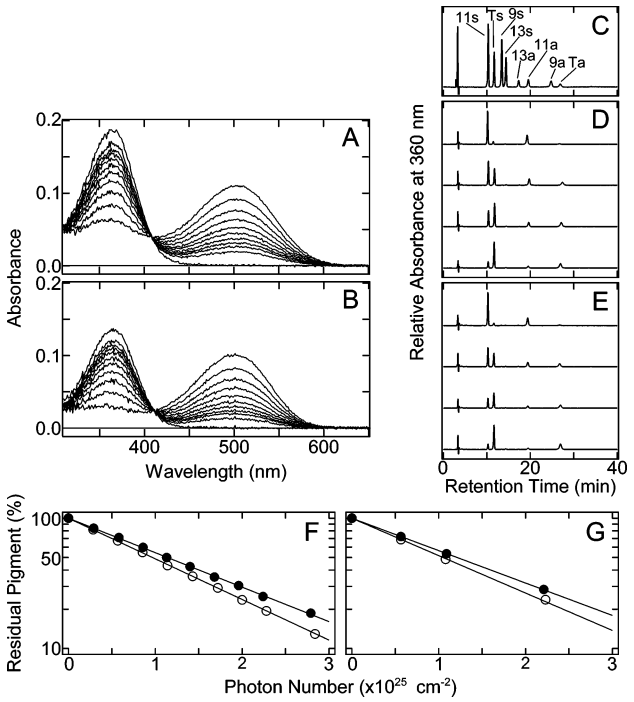

FIGURE 3: Photosensitivity of the protonated form (pH 5.5) of the rhodopsin E113Q mutant. (A) The photosensitivity of the rhodopsin E113Q mutant was measured at pH 5.5 using UV−vis spectrophotometry. The sample was irradiated successively with 500 nm light, and absorbance changes were monitored. The sample was completely bleached at the end of the experiment. (B) The photosensitivity of the wild type was measured at the same time as a reference in every experiment. The same set of experiments was performed four times to calculate the standard deviation, but only one representative set of data is shown. (C−E) The photosensitivity of the protonated form of the E113Q mutant was measured also by chromophore extraction followed by HPLC analysis. The samples of the protonated form were irradiated with 500 nm light for 0, 5, 10, or 20 min in the presence of 4.8 mM hydroxylamine. Chromophores were extracted from irradiated samples as retinaloximes and then subjected to HPLC analysis. Again, the photosensitivity of the wild type was measured at the same time as a reference in every experiment. (C) The HPLC pattern of a sample containing authentic *syn* and *anti* isomers of 11-*cis*-, 9-*cis*-, 13-*cis*-, and *all-trans*-retinaloximes: 13s, 13-*cis*-15-*syn*-retinaloxime; 13a, 13-*cis*-15-*anti*-retinaloxime; 11s, 11-*cis*-15-*syn*-retinaloxime; 11a, 11-*cis*-15-*anti*-retinaloxime; 9s, 9-*cis*-15-*syn*-retinaloxime; 9a, 9-*cis*-15-*anti*-retinaloxime; Ts, *all-trans*-15-*syn*-retinaloxime; Ta, *all-trans*-15-*anti*-retinaloxime. (D, E) The HPLC patterns of the protonated form of the E113Q mutant (D) and of wild-type rhodopsin (E) (0, 5, 10, and 20 min irradiation from the top of the each panel). The same set of experiments was repeated four times, but only one representative set of data is shown. It is clearly shown that photoisomerization from the 11-*cis* to all-*trans* form took place as a function of irradiation time. The isomeric compositions of the samples were calculated from the areas of the peaks and the molar extinction coefficients of retinaloximes at 360 nm. (F, G) The amounts of residual pigment determined were plotted on a semilogarithmic scale against the incident photon flux. (F) UV−vis spectrophotometry. (G) HPLC. A representative plot (the same experiment as in panels A, B, D, and E) out of four experiments for each method is shown. Open and solid circles represent the wild type and the protonated form of the E113Q mutant, respectively. The photosensitivity of the mutant, which was estimated as the slope of the fitting line, was 0.87 ± 0.02 (n = 4) relative to the wild type.

amounts of residual pigment were calculated, after the correction for dark bleaching, from the percentages of the 11-*cis* isomer in each sample. The data were then plotted against incident photon number and fitted with an exponential function (Figure 3G). The photosensitivity of the pigment was determined as a relative value to that of wild-type rhodopsin, which was measured at the same time in every experiment. The photosensitivity was estimated to be 0.87 ± 0.02 (n = 4) relative to the wild type. The good agreement of the value with that determined by UV−vis spectrophotometry (0.87 ± 0.02) validates this method. The quantum yield was calculated to be 0.65 ± 0.02.

Quantum Yield of the UV Pigments. Before our photosensitivity measurements of the UV pigments, we confirmed that photoisomerization of *all-trans*-retinaloxime by the UV light was negligible under the conditions that the photosensitivities were measured. Namely, the sample of wild-type rhodopsin was first completely bleached by intense >500 nm light in the presence of hydroxylamine to produce *all-trans*-retinaloxime, and the sample was then irradiated with 359 nm light for 0 or 100 min, followed by chromophore extraction and HPLC analysis. Both the 0 and 100 min samples contained ∼90% of the all-*trans* isomer and exhibited almost identical isomeric compositions (Figure 4B), indicating that photoisomerization by 359 nm light had not taken place under these conditions. This high photostability of retinaloxime is consistent with the experimental observation that *all-trans*-retinaloxime was not isomerized to much extent (6−23%) even by the 3 h irradiation with a 30 W fluorescent lamp in any organic solvent, as opposed to retinal which underwent 40−80% isomerization by the 30 min irradiation (*36*).

We also estimated the stability of the pigments against hydroxylamine. Namely, a sample was divided into two aliquots, and each was acid denatured after incubation with hydroxylamine (the unprotonated form, 2.4 mM; mouse UV, 9.5 mM) for 0 min or ∼15 h (data not shown). Using the estimated amount of residual pigment after the ∼15 h incubation, the rate constant of the bleaching was calculated to be (3.3 ± 1.7) × 10^{-4} min^{-1} (n = 3) for the unprotonated form and (1.1 ± 0.2) × 10^{-4} min^{-1} (n = 2) for mouse UV. These values were used in the correction to the photobleaching data (see Supporting Information).

The samples of the unprotonated form were irradiated with 390 nm light for 0, 5, 10, or 20 min in the presence of 2.4 mM hydroxylamine. Chromophores were extracted from the irradiated samples as retinaloximes and subjected to HPLC analysis (Figure 4C). Again, the photoisomerization from the 11-*cis* to all-*trans* form took place as a function of irradiation time, and small amounts of 9-*cis* and 13-*cis* isomers (<5% in total) were present in the extracts. The amounts of residual pigment were calculated, after the correction for dark bleaching, from the percentages of 11-*cis* isomer in each sample. The data were then plotted against incident photon number and fitted with an exponential function (Figure 4E). The photosensitivity of the pigment was determined relative to that of wild-type rhodopsin, which was measured at the same time in every experiment. The photosensitivity of the unprotonated form was 0.61 ± 0.03 (n = 4) relative to the wild type. Using this value and the molar extinction coefficient at 390 nm (38100 ± 1000 M^{-1} cm^{-1}), the quantum yield of the unprotonated form was calculated to be 0.42 ± 0.02, which was significantly lower than that of the wild type [0.65 (*18*)]. It should be noted that the quantum yields of the wild type at pH 5.5 or pH 8.2 were almost identical to that at pH 6.5 (Table 1).

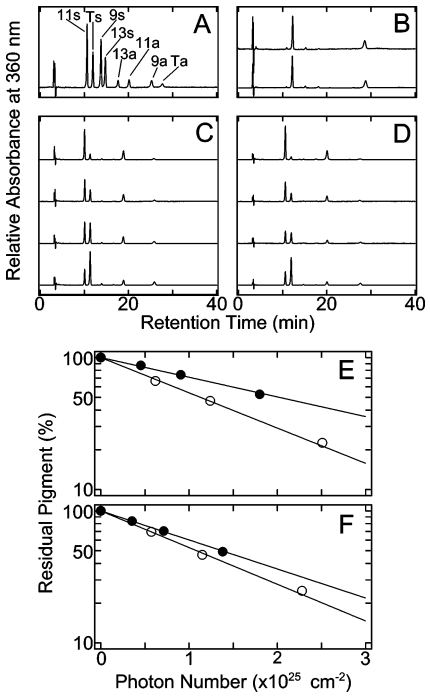

FIGURE 4: Photosensitivities of UV pigments. (A) The HPLC pattern of the authentic sample. (B) The sample containing *all-trans*-retinaloxime was irradiated with 359 nm light for 0 or 100 min, followed by chromophore extraction and HPLC analysis. The HPLC pattern of the irradiated sample (lower trace) was almost identical to that of the nonirradiated sample (upper trace), indicating that photoisomerization of *all-trans*-retinaloxime by 359 nm light does not take place in these conditions. (C, D) The photosensitivities of UV pigments, the unprotonated form (pH 8.2) of the rhodopsin E113Q mutant and mouse UV, were measured by chromophore extraction followed by HPLC analysis. The procedures were the same as the measurement of the protonated form of the E113Q mutant, except for the final concentration of hydroxylamine (the unprotonated form, 2.4 mM; mouse UV, 9.5 mM) and the wavelength of irradiation (the unprotonated form, 390 nm; mouse UV, 359 nm). The photosensitivity of wild-type rhodopsin at 500 nm was measured at the same time as a reference in every experiment. The HPLC patterns of the unprotonated form of the rhodopsin E113Q mutant (C) and mouse UV (D) are shown (0, 5, 10, and 20 min irradiation from the top of the each panel). The same set of experiments was repeated four times for each pigment, but only one representative data set for each pigment is shown. (E, F) The amounts of residual pigments were plotted on a semilogarithmic scale against the incident photon flux (E, the unprotonated form of the rhodopsin E113Q mutant; F, mouse UV; the same experiments as in panels C and D). Open circles represent wild-type rhodopsin, and solid circles represent the unprotonated form of the E113Q mutant or mouse UV in panel E or F, respectively. The photosensitivities relative to wild-type rhodopsin were estimated to be 0.61 ± 0.03 ($n = 4$) and 0.84 ± 0.06 ($n = 4$) for the rhodopsin mutant and mouse UV, respectively.

The photosensitivity of mouse UV was measured in the presence of 9.5 mM hydroxylamine. The samples were irradiated by 359 nm light in the same way as the unprotonated form, followed by chromophore extraction and HPLC analysis (Figure 4D). The amounts of residual pigments were plotted on a semilogarithmic scale against the incident photon flux and fitted with an exponential function (Figure 4F). The photosensitivity was 0.84 ± 0.06 ($n = 4$) relative to wild-type rhodopsin. Using the photosensitivity and the molar extinction coefficient at 359 nm (43600 ± 1200 M^{-1} cm^{-1}), the quantum yield of mouse UV was calculated to be 0.51 ± 0.04, which was about 80% of that of wild-type rhodopsin. It is noteworthy that the value is significantly higher than that of the unprotonated form of the rhodopsin E113Q mutant (0.42 ± 0.02). All results are summarized in Figure 5 and Table 1.

DISCUSSION

In the present study, we determined the quantum yields of the protonated and unprotonated form of the bovine rhodopsin E113Q mutant and the mouse UV pigment (mouse UV). To our knowledge, this is the first direct determination of the quantum yield of visual pigments that have unprotonated Schiff base chromophores.

The quantum yield of the rhodopsin E113Q mutant was much lower at pH 8.2 than at pH 5.5. This result is consistent with the notion described in the report of Lewis et al. (*41*). That is, they estimated the relative quantum yields of the E113Q mutant at pH 5.5 and 8.2, based on the amount of batho formation, and reported that the quantum yield of the unprotonated form was smaller and "the difference was less than a factor of 2". On the other hand, Fahmy and Sakmar (*42*) stated that the quantum yield of the unprotonated form of the E113Q mutant was comparable to that of the protonated form, based on a comparison between the wavelength profile of the transducin activation efficiency and the absorption spectrum at pH 6.2. However, their results showed that the transducin activation rate was higher for light in the visible than for light in the UV, whereas the absorption spectrum was higher in the UV region than in the visible region (or at least comparable in both regions even if the scattering effect at shorter wavelengths is taken into account), suggesting that the quantum yield of the unprotonated form could be lower than the protonated form. In any case, these results including ours suggest that the Schiff base protonation contributes to the photoisomerization efficiency.

A comprehensive study on the quantum yield of 11-*cis*-retinal Schiff base in solution by Becker and Freedman (*20*) revealed that the quantum yield was strongly dependent on the solvent polarity, from ≤ 0.01 in hexane to ~ 0.20 in polar solvents such as dichloromethane, acetone, and methanol. They also argued that, on the basis of the fact that the quantum yield in acetonitrile was 0.34, the quantum yield of the unprotonated Schiff base was greatly enhanced by the hydrogen-bonding capacity of solvent. On the other hand, the quantum yield of the protonated Schiff base of retinal was independent of the solvent polarity or hydrogen-bonding capacity, because its value in various solvents was almost constant (~ 0.20). These results were accounted for as follows: Protonation or solvent polarity/hydrogen-bonding capacity caused a mixing (or a reversal of the level ordering) of two low-lying singlet excited states (Bu^+-like and Ag^--like states), resulting in elimination of the barrier for photoisomerization. Although a later study on the fluorescence properties of the unprotonated Schiff base of *all-trans*-retinal at room temperature argued that polarity-dependent mixing of the singlet states was not likely to occur (*43*), it is certain that the excited-stated dynamics of the unprotonated Schiff base are remarkably different from those of the protonated Schiff base. For example, the change of dipole moment upon excitation of the unprotonated Schiff base is smaller than that for the protonated Schiff base (*44*, *45*). Considering the potential importance of charge translocation along the chromophore in the photoisomerization process

Table 1: Experimental Conditions and Photoreactive Properties of Visual Pigments

pigment	pH	λ_{max}[a] (nm)	method[b]	C_{NH_2OH}[c] (mM)	λ_{irrad}[d] (nm)	ϵ_{irrad}[e] (M^{-1} cm^{-1})	S[f]	ϕ[g]
bRh[h] wild type	6.5	500	UV−vis/ HPLC	48	500	40600[i]	1.00	0.65[j]
	5.5	500	UV−vis	48	500	41900	1.03	0.65
	8.2	500	UV−vis	48	500	41700	1.05	0.66
bRh E113Q	5.5	500	UV−vis	4.8	500	35600 (1000)[k]	0.87 (0.02)	0.65 (0.02)
			HPLC	4.8	500		0.87 (0.02)	0.65 (0.02)
	8.2	385	HPLC	2.4	390	38100 (1000)	0.61 (0.03)	0.42 (0.02)
mUV[l]	6.5	358	HPLC	9.5	359	43600 (1200)	0.84 (0.06)	0.51 (0.04)

[a] Wavelength at the absorption maximum. [b] Method for estimating the photosensitivity. [c] Final concentration of hydroxylamine used in the photosensitivity measurement. [d] Irradiation wavelength. [e] Molar extinction coefficient at λ_{irrad}. [f] Photosensitivity at λ_{irrad} (relative to wild-type bovine rhodopsin). [g] Quantum yield at λ_{irrad}. [h] Bovine rhodopsin. [i] Reference *39*. [j] Reference *18*. [k] The values in parentheses are standard deviations calculated from at least four independent experiments. [l] Mouse UV.

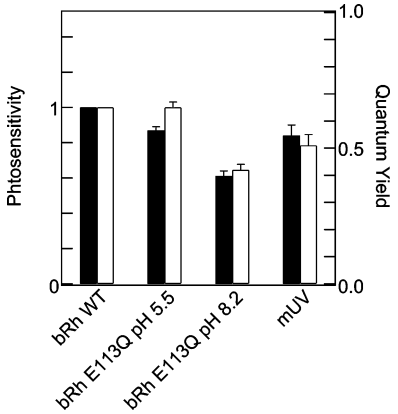

FIGURE 5: Summary of the photosensitivities and the quantum yields of visual pigments. The photosensitivities are shown in filled bars, and the quantum yields are shown in open bars. The left and right axes are graduated in the photosensitivity and the quantum yield, respectively. Error bars represent the standard deviations calculated from four independent experiments for each pigment. Abbreviations: bRh, bovine rhodopsin; WT, wild type; mUV, mouse UV.

(*46*), this may be one of the reasons for the less efficient photoisomerization of the unprotonated Schiff base in nonpolar solvent as well as in the rhodopsin E113Q mutant. In addition, the fluorescence lifetime of the unprotonated Schiff base of *all-trans*-retinal in solutions with different polarities (20−100 ps) is longer than that of the protonated Schiff base (<5−7 ps) (*43*). This observation suggests that the excited-state lifetime of the unprotonated Schiff base is longer than the protonated one; hence isomerization takes place more slowly.

It is likely that intrinsic properties of the unprotonated Schiff base that differ from those of the protonated Schiff base are responsible for the lower quantum yield in the rhodopsin E113Q mutant at the basic pH. However, we cannot exclude the possibility that the E113Q mutation affected the photoisomerization efficiency through changes of the conformation and/or the hydrogen-bonding network of the binding pocket. In addition, the loss of a point negative charge may be responsible for the less efficient photoisomerization. Additional experiments are required to test those possibilities.

The quantum yield of the unprotonated form of the E113Q mutant observed here (0.42 ± 0.02) is higher than that of the free unprotonated Schiff base in solution (~0.20 in polar solvents) (*20*), although it is significantly lower than those of the other pigments investigated here. This observation implies that the protein facilitates photoisomerization through other mechanisms than the protonation of the Schiff base, such as a fixing of the chromophore at both ends (*47*), a pretwist of the isomerizing C11═C12 bond (*48*), intramolecular or intermolecular interactions of methyl groups of the chromophore (*49*), and an inhibition of unreactive motions (*22*). It has also been proposed that the efficient photoisomerization is an intrinsic property of the chromophore and the protein offers a gas-phase-like (i.e., free from the medium effect) environment rather than specific interactions to enhance the reactivity (*50*).

The relative photosensitivity of mouse UV determined here (0.84 ± 0.06) is lower than that of rhodopsin (1.00) and iodopsin, the chicken red-sensitive cone pigment (1.08 ± 0.02) (*26*). This result is apparently inconsistent with the earlier study of Makino and Dodd, who reported that, on the basis of the measurements of early receptor currents of salamander cones, the photosensitivity of UV cone pigment was ~1.4 times higher than that of red cone pigment (*51*). The discrepancy may be due to a difference of animal species, the presence of A2 retinal in salamander pigments, or the differences in the conditions and methods. It should be noted that our value was determined by a more direct method.

The higher quantum yield of mouse UV than the unprotonated form of the rhodopsin E113Q mutant suggests that mouse UV has a specific mechanism for efficient photoisomerization of the unprotonated Schiff base. Therefore, elucidation of the mechanism of efficient photoisomerization of the unprotonated Schiff base in mouse UV by comprehensive site-directed mutagenesis will be our future investigation.

ACKNOWLEDGMENT

We thank Dr. S. Koike for providing us with the HEK 293T cell line, Prof. F. Tokunaga for providing us with a pUSRα expression vector, and Prof. R. S. Molday for the generous gift of a Rho1D4-producing hybridoma. We are also grateful to Dr. S. Kuwayama for technical advice, Drs. A. Terakita, Y. Imamoto, and T. Yamashita for valuable discussions, and Prof. T. G. Ebrey for critical reading of the manuscript and invaluable comments.

SUPPORTING INFORMATION AVAILABLE

The method of a correction for the bleaching of the pigment in the dark due to reaction with hydroxylamine. This material is available free of charge via the Internet at http://pubs.acs.org.

REFERENCES

1. Yoshizawa, T., and Wald, G. (1963) Pre-lumirhodopsin and the bleaching of visual pigments, *Nature 197*, 1279−1286.
2. Kandori, H., Shichida, Y., and Yoshizawa, T. (2001) Photoisomerization in rhodopsin, *Biochemistry (Moscow) 66*, 1197−1209.
3. Schoenlein, R. W., Peteanu, L. A., Mathies, R. A., and Shank, C. V. (1991) The first step in vision: femtosecond isomerization of rhodopsin, *Science 254*, 412−415.
4. Shichida, Y., and Imai, H. (1998) Visual pigment: G-protein-coupled receptor for light signals, *Cell. Mol. Life Sci. 54*, 1299−1315.
5. Okano, T., Kojima, D., Fukada, Y., Shichida, Y., and Yoshizawa, T. (1992) Primary structures of chicken cone visual pigments: vertebrate rhodopsins have evolved out of cone visual pigments, *Proc. Natl. Acad. Sci. U.S.A. 89*, 5932−5936.
6. Yokoyama, S. (2000) Molecular evolution of vertebrate visual pigments, *Prog. Retinal Eye Res. 19*, 385−419.
7. Ebrey, T., and Koutalos, Y. (2001) Vertebrate photoreceptors, *Prog. Retinal Eye Res. 20*, 49−94.
8. Harosi, F. I. (1994) An analysis of two spectral properties of vertebrate visual pigments, *Vision Res. 34*, 1359−1367.
9. Lewis, A., Fager, R. S., and Abrahamson, E. W. (1973) Tunable laser resonance Raman spectroscopy of the visual process. I: The spectrum of rhodopsin, *J. Raman Spectrosc. 1*, 465−470.
10. Oseroff, A. R., and Callender, R. H. (1974) Resonance Raman spectroscopy of rhodopsin in retinal disk membranes, *Biochemistry 13*, 4243−4248.
11. Fasick, J. I., Applebury, M. L., and Oprian, D. D. (2002) Spectral tuning in the mammalian short-wavelength sensitive cone pigments, *Biochemistry 41*, 6860−6865.
12. Dukkipati, A., Kusnetzow, A., Babu, K. R., Ramos, L., Singh, D., Knox, B. E., and Birge, R. R. (2002) Phototransduction by vertebrate ultraviolet visual pigments: protonation of the retinylidene Schiff base following photobleaching, *Biochemistry 41*, 9842−9851.
13. Kawamura, S., and Yokoyama, S. (1998) Functional characterization of visual and nonvisual pigments of American chameleon (*Anolis carolinensis*), *Vision Res. 38*, 37−44.
14. Yokoyama, S., Radlwimmer, F. B., and Kawamura, S. (1998) Regeneration of ultraviolet pigments of vertebrates, *FEBS Lett. 423*, 155−158.
15. Wilkie, S. E., Vissers, P. M., Das, D., Degrip, W. J., Bowmaker, J. K., and Hunt, D. M. (1998) The molecular basis for UV vision in birds: spectral characteristics, cDNA sequence and retinal localization of the UV-sensitive visual pigment of the budgerigar (*Melopsittacus undulatus*), *Biochem. J. 330* (Part 1), 541−547.
16. Becker, R. S. (1988) The visual process: photophysics and photoisomerization of model visual pigments and the primary reaction, *Photochem. Photobiol. 48*, 369−399.
17. Birge, R. R. (1990) Nature of the primary photochemical events in rhodopsin and bacteriorhodopsin, *Biochim. Biophys. Acta 1016*, 293−327.
18. Kim, J. E., Tauber, M. J., and Mathies, R. A. (2001) Wavelength dependent cis-trans isomerization in vision, *Biochemistry 40*, 13774−13778.
19. Dartnall, H. J. (1968) The photosensitivities of visual pigments in the presence of hydroxylamine, *Vision Res. 8*, 339−358.
20. Becker, R. S., and Freedman, K. (1985) Comprehensive investigation of the mechanism and photophysics of isomerization of a protonated and unprotonated Schiff base of 11-*cis*-retinal, *J. Am. Chem. Soc. 107*, 1477−1485.
21. Mizukami, T., Kandori, H., Shichida, Y., Chen, A. H., Derguini, F., Caldwell, C. G., Biffe, C. F., Nakanishi, K., and Yoshizawa, T. (1993) Photoisomerization mechanism of the rhodopsin chromophore: picosecond photolysis of pigment containing 11-cis-locked eight-membered ring retinal, *Proc. Natl. Acad. Sci. U.S.A. 90*, 4072−4076.
22. Liu, R. S., and Colmenares, L. U. (2003) The molecular basis for the high photosensitivity of rhodopsin, *Proc. Natl. Acad. Sci. U.S.A. 100*, 14639−14644.
23. Zhukovsky, E. A., and Oprian, D. D. (1989) Effect of carboxylic acid side chains on the absorption maximum of visual pigments, *Science 246*, 928−930.
24. Sakmar, T. P., Franke, R. R., and Khorana, H. G. (1989) Glutamic acid-113 serves as the retinylidene Schiff base counterion in bovine rhodopsin, *Proc. Natl. Acad. Sci. U.S.A. 86*, 8309−8313.
25. Nathans, J. (1990) Determinants of visual pigment absorbance: identification of the retinylidene Schiff's base counterion in bovine rhodopsin, *Biochemistry 29*, 9746−9752.
26. Okano, T., Fukada, Y., Shichida, Y., and Yoshizawa, T. (1992) Photosensitivities of iodopsin and rhodopsins, *Photochem. Photobiol. 56*, 995−1001.
27. Nathans, J. (1990) Determinants of visual pigment absorbance: role of charged amino acids in the putative transmembrane segments, *Biochemistry 29*, 937−942.
28. Onishi, A., Hasegawa, J., Imai, H., Chisaka, O., Ueda, Y., Honda, Y., Tachibana, M., and Shichida, Y. (2005) Generation of knock-in mice carrying third cones with spectral sensitivity different from S and L cones, *Zool. Sci. 22*, 1145−1156.
29. Oprian, D. D., Asenjo, A. B., Lee, N., and Pelletier, S. L. (1991) Design, chemical synthesis, and expression of genes for the three human color vision pigments, *Biochemistry 30*, 11367−11372.
30. Nagata, T., Terakita, A., Kandori, H., Kojima, D., Shichida, Y., and Maeda, A. (1997) Water and peptide backbone structure in the active center of bovine rhodopsin, *Biochemistry 36*, 6164−6170.
31. Kayada, S., Hisatomi, O., and Tokunaga, F. (1995) Cloning and expression of frog rhodopsin cDNA, *Comp. Biochem. Physiol., Part B: Biochem. Mol. Biol. 110*, 599−604.
32. Takebe, Y., Seiki, M., Fujisawa, J., Hoy, P., Yokota, K., Arai, K., Yoshida, M., and Arai, N. (1988) SR alpha promoter: an efficient and versatile mammalian cDNA expression system composed of the simian virus 40 early promoter and the R-U5 segment of human T-cell leukemia virus type 1 long terminal repeat, *Mol. Cell. Biol. 8*, 466−472.
33. Sakmar, T. P., Franke, R. R., and Khorana, H. G. (1991) The role of the retinylidene Schiff base counterion in rhodopsin in determining wavelength absorbance and Schiff base pK_a, *Proc. Natl. Acad. Sci. U.S.A. 88*, 3079−3083.
34. Shichida, Y., Nakamura, K., Yoshizawa, T., Trehan, A., Denny, M., and Liu, R. S. (1988) 9,13-dicis-rhodopsin and its one-photon-one-double-bond isomerization, *Biochemistry 27*, 6495−6499.
35. Imamoto, Y., Yoshizawa, T., and Shichida, Y. (1996) Chromophore configuration of iodopsin and its photoproducts formed at low temperatures, *Biochemistry 35*, 14599−14607.
36. Tsukida, K., Ito, M., Tanaka, T., and Yagi, I. (1985) High-performance liquid chromatographic and spectroscopic characterization of stereoisomeric retinaloximes Improvements in resolution and implications of the method, *J. Chromatogr. 331*, 265−272.
37. Trehan, A., Liu, R. S. H., Shichida, Y., Imamoto, Y., Nakamura, K., and Yoshizawa, T. (1990) On retention of chromophore configuration of rhodopsin isomers derived from three dicis retinal isomers, *Bioorg. Chem. 18*, 30−40.
38. Fasick, J. I., Lee, N., and Oprian, D. D. (1999) Spectral tuning in the human blue cone pigment, *Biochemistry 38*, 11593−11596.
39. Wald, G., and Brown, P. K. (1953) The molar extinction of rhodopsin, *J. Gen. Physiol. 37*, 189−200.
40. Gross, A. K., Rao, V. R., and Oprian, D. D. (2003) Characterization of rhodopsin congenital night blindness mutant T94I, *Biochemistry 42*, 2009−2015.
41. Lewis, J. W., Szundi, I., Fu, W. Y., Sakmar, T. P., and Kliger, D. S. (2000) pH dependence of photolysis intermediates in the photoactivation of rhodopsin mutant E113Q, *Biochemistry 39*, 599−606.
42. Fahmy, K., and Sakmar, T. P. (1993) Light-dependent transducin activation by an ultraviolet-absorbing rhodopsin mutant, *Biochemistry 32*, 9165−9171.
43. Bachilo, S. M., Bondarev, S. L., and Gillbro, T. (1996) Fluorescence properties of protonated and unprotonated Schiff bases of retinal at room temperature, *J. Photochem. Photobiol. B 34*, 39−46.
44. Mathies, R., and Stryer, L. (1976) Retinal has a highly dipolar vertically excited singlet state: implications for vision, *Proc. Natl. Acad. Sci. U.S.A. 73*, 2169−2173.
45. Hufen, J., Sugihara, M., and Buss, V. (2004) How the counterion affects ground- and excited-state properties of the rhodopsin chromophore, *J. Phys. Chem. B 108*, 20419−20426.
46. Schenkl, S., van Mourik, F., van der Zwan, G., Haacke, S., and Chergui, M. (2005) Probing the ultrafast charge translocation of photoexcited retinal in bacteriorhodopsin, *Science 309*, 917−920.
47. Freedman, K., Becker, R. S., Hannak, D., and Bayer, E. (1986) Investigation into the spectroscopy and photoisomerization of a

series of poly(ethylene glycol) peptide Schiff bases of 11-cis retinal, *Photochem. Photobiol. 43*, 291−295.
48. Okada, T., Sugihara, M., Bondar, A. N., Elstner, M., Entel, P., and Buss, V. (2004) The retinal conformation and its environment in rhodopsin in light of a new 2.2 Å crystal structure, *J. Mol. Biol. 342*, 571−583.
49. Kochendoerfer, G. G., Verdegem, P. J., van der Hoef, I., Lugtenburg, J., and Mathies, R. A. (1996) Retinal analog study of the role of steric interactions in the excited state isomerization dynamics of rhodopsin, *Biochemistry 35*, 16230−16240.
50. Cembran, A., Bernardi, F., Olivucci, M., and Garavelli, M. (2005) The retinal chromophore/chloride ion pair: structure of the photoisomerization path and interplay of charge transfer and covalent states, *Proc. Natl. Acad. Sci. U.S.A. 102*, 6255−6260.
51. Makino, C. L., and Dodd, R. L. (1996) Multiple visual pigments in a photoreceptor of the salamander retina, *J. Gen. Physiol. 108*, 27−34.

BI7003763